Wavy-to-Slug Flow Transition in Slightly Inclined Gas–Liquid Pipe Flow

Eric Grolman, Niels C. J. Commandeur, Eduard C. de Baat, and Jan M. H. Fortuin
Dept. of Chemical Engineering, University of Amsterdam, 1018 WV Amsterdam, The Netherlands

A process-engineering model is presented for the stratified-wavy-to-intermittent (SW – I) flow-pattern transition in slightly inclined gas – liquid pipe flow. The main parameter for predicting (in)stability of wavy flow in inclined pipes is the average liquid holdup, which was found to reach a maximum, critical value at flow-pattern transition. Observed values of the critical liquid holdup vary between 0.07 and 0.42, depending on pipe diameter, angle of inclination and transport properties of the gas – liquid system. Measurements were performed in transparent glass pipes of 26- and 51-mm dia., at ten angles of inclination ($0.1° \leq \beta \leq 6.0°$), using air/water and air/tetradecane ($n\text{-}C_{14}H_{30}$) systems at atmospheric pressure. Flow-pattern maps are presented for selected angles of inclination, showing excellent agreement between predicted and observed flow-pattern boundaries.

Introduction

In *upward* inclined sections of pipelines carrying gas and liquid simultaneously, liquid may accumulate when the gas velocity is insufficient to advance the liquid against the opposing action of gravity. The accumulation of liquid eventually leads to periodic pipe blockage, that is, *slug* or *semislug* flow. In semislug flow the slugs are highly aerated. Although the complete circumference of the pipe is periodically wetted, the gas phase remains to some extent continuous. In gas–liquid pipe flow slugs and semislugs should often be avoided for reasons of safety, increased average axial pressure gradient, oscillating pressure, oscillating liquid production, possible damage to downstream equipment, and so forth. Models that predict the stratified-wavy-to-intermittent (SW-I) (slug or semislug) flow-pattern transition are important for the design, scale-up, and control of two-phase pipelines. The present study shows that angles of inclination as small as $+0.1°$ can cause severe slugging. Because commercial pipelines generally cannot be constructed to within 0.1° accuracy in the angle of inclination, the possible occurrence of slugs should generally be anticipated.

Correspondence concerning this article should be addressed to J. M. H. Fortuin.
Current address of E. Grolman: Faculty of Chemical Technology and Materials Science, Delft University of Technology, Julianalaan 136, 2628 BL Delft, N. L.

Existing Models for the Stratified-Wavy-to-Intermittent Transition

The SW-I flow-pattern transition is generally thought to occur when high waves on the gas–liquid interface grow exponentially and bridge the gas core. The transition has been studied extensively in *horizontal* pipes and channels. Kelvin (1871) and Helmholtz (1868) presented a theoretical analysis of the growth of small, inviscid waves on gas-sheared liquid layers of infinite depth, resulting in a critical gas velocity for the onset of waves and slugs. Kordyban and Ranov (1970) performed experiments in a rectangular channel and obtained a criterion for the onset of slug flow, containing the wave number. However, the prediction of wave characteristics, such as the wave number, for gas–liquid pipe flow is a complicated matter still under investigation and cannot be relied upon (Bruno and McCready, 1989).

It is generally recognized that the original Kelvin–Helmholtz criterion predicts critical gas velocities that are too high for the onset of both waves and slugs. To obtain better agreement with experimental data, the criterion was modified with an empirical constant $c_{K\text{-}H}$ by various authors. The (modified) Kelvin–Helmholtz criteria are summarized in Eq. 1.

$$u_G - u_L \geq c_{K\text{-}H}\sqrt{(\rho_L - \rho_G)gh_G/\rho_G} \tag{1}$$

with

$c_{K\text{-}H} = 1.0$; Kelvin (1871)–Helmholtz (1868)

$c_{K\text{-}H} = 0.5$; Wallis and Dobson (1973)

$c_{K\text{-}H} = 0.74$; Kordyban (1977), with h_G at the wave top

$c_{K\text{-}H} = 0.487$; Mishima and Ishii (1980).

Taking h_G to be the *average* height of the air passage, Wallis and Dobson (1973) obtained $c_{K\text{-}H} = 0.5$ on empirical grounds. Mishima and Ishii (1980) used long-wave approximations in a linear stability analysis and obtained $c_{K\text{-}H} = 0.487$. Contrary to the other authors listed here, Kordyban (1977) took h_G at the wave top, resulting in the different value, $c_{K\text{-}H} = 0.74$.

Taitel and Dukler (1976) extended the Kelvin–Helmholtz theory to pipes of circular cross section and waves of finite amplitude. They obtained

$$u_G \geq (1 - h_L/D)\sqrt{\frac{(\rho_L - \rho_G) g \cos(\beta) A_G}{\rho_G \mathrm{d}A_L/\mathrm{d}h_L}} \qquad (2)$$

where A_L and A_G are the liquid and gas-phase cross-sectional areas, and h_L is the average liquid layer depth, measured vertically through the centerline of the pipe.

Wallis (1969) derived conditions for wave instability, predicting exponential wave growth when the *continuity* wave velocity *exceeds* the *dynamic* wave velocity. This condition has led some authors to the conclusion that intermittent flow can only be initiated in *supercritical* flow, that is, when the bulk liquid velocity is larger than the velocity of interfacial waves relative to the liquid (Taitel and Dukler, 1977). Our experiments conducted at low liquid velocities ($u_L < 0.01$ m·s^{-1}), that is, under *subcritical* conditions, demonstrate without doubt, that supercritical flow is not a prerequisite for the onset of slug flow in inclined pipes.

The equations of continuity and motion of gas and liquid, for the direction of mass flow, were solved numerically by Barnea and Taitel (1989, 1993), using linear approximations. The resulting (in)stability criteria for interfacial waves are similar to those of Wallis (1969), except for additional terms and factors due to the circular (pipe) geometry and the inclusion of the surface tension σ.

A rather complete one-dimensional linear stability analysis of gas–liquid flow in both rectangular channels and pipes of circular cross section was presented by Lin and Hanratty (1986). This analysis includes shear-stress and pressure fluctuations in phase with the wave slope and in phase with the wave height. However, the validity of this and less involved linear theories, at superficial gas velocities above 3.3 m·s^{-1} and in larger diameter pipes, is questionable (Hanratty, 1991).

In the literature today, no distinction is made between modeling stability in *horizontal* and in *inclined* gas–liquid pipe flow. Although the criteria just listed were developed for horizontal gas–liquid flow, their application is extended to inclined flow as the necessity arises (Taitel and Dukler, 1976; Barnea and Taitel, 1993). However, increasingly accurate laboratory experiments in inclined pipes have revealed a demand for better stability criteria, so that predictions approaching the limits of experimental uncertainty can be obtained.

The Model for the Stratified-Wavy-to-Intermittent Flow-Pattern Transition

In inclined pipes, across a fairly large range of (small) liquid flow rates, the SW-I flow-pattern boundary is approached by decreasing the superficial gas velocity until intermittent flow occurs. Certain combinations of gas flow rate and liquid holdup are marginally stable, so that a small reduction in gas flow rate leads to exponential growth of the liquid holdup and the development of a liquid slug. The usual method for defining such an instability is to impose a requirement of infinite gradient, which for the system considered reads: $\partial\epsilon_L/\partial u_{GS} \to -\infty$. However, the liquid holdup is physically limited to values between zero and one. Consequently, the maximum change in holdup, $\Delta\epsilon_{L,\max}$, that can be achieved is equal to one. When the pipe is suddenly blocked by the liquid phase at the SW-I flow pattern transition, the superficial gas velocity drops from an initial value of u_{GS}, to a value of zero in the liquid slug. Therefore, the change in superficial gas velocity that corresponds to the *maximum* change in liquid holdup is equal to $-u_{GS}$. It must be concluded that there exists a physical limit to the value of $-\partial\epsilon_L/\partial u_{GS}$, which is given by

$$-\frac{\partial\epsilon_L}{\partial u_{GS}} \leq \frac{-\Delta\epsilon_{L,\max}}{\Delta u_{GS}} = \frac{0-1}{0-u_{GS}} = \frac{1}{u_{GS}}.$$

We propose that an instability occurs when $\partial\epsilon_L/\partial u_{GS}$ surpasses a *finite* threshold value, which is equal to a certain fraction a of the physically limiting value $(\Delta\epsilon_{L,\max}/\Delta u_{GS}) = -1/u_{GS}$. This assumption leads to the following general relationship between $\epsilon_{L,\text{SW-I}}$ and u_{GS}, that is, between the critical liquid holdup at conditions of marginal stability and the superficial gas velocity, respectively:

$$\frac{\partial\epsilon_{L,\text{SW-I}}}{\partial u_{GS}} = -\frac{a}{u_{GS}}. \qquad (3)$$

Integration of Eq. 3 with boundaries running from $u_{GS} = u_{G0}$ to u_{GS} results in the following general equation for $\epsilon_{L,\text{SW-I}}$:

$$\epsilon_{L,\text{SW-I}} = \epsilon_{L0} - a \ln\frac{u_{GS}}{u_{G0}}, \qquad a = 0.21; \qquad \epsilon_{L0} = 0.486;$$

$$u_{G0} \equiv \left\{ \nu_G^2 \left(\frac{\rho_L}{\rho_G} - 1 \right)^3 g^3 D \right\}^{1/8}. \qquad (4)$$

The constants a and ϵ_{L0} were determined from semilogarithmic plots of ϵ_L vs. u_{GS}/u_{G0} (Figure 1), using the results of all 1270 experiments close to and on the SW-I transition. The variation of $\epsilon_{L,\text{SW-I}}$ with pipe diameter and liquid-phase transport properties were successfully incorporated into the parameter u_{G0}. Dimensional consistency of u_{G0} has led to the inclusion of the parameters ρ_G, ν_G, and g in the definition, none of which were varied. The gas–liquid interfacial tension σ and liquid-phase viscosity η_L were varied by using both a water and a tetradecane liquid phase. Although these transport properties do have an effect on the steady-state liquid holdup, ϵ_L, no effects of σ and η_L on $\epsilon_{L,\text{SW-I}}$ were found. For the atmospheric flow of *air* and *water* in a 51-mm-dia.

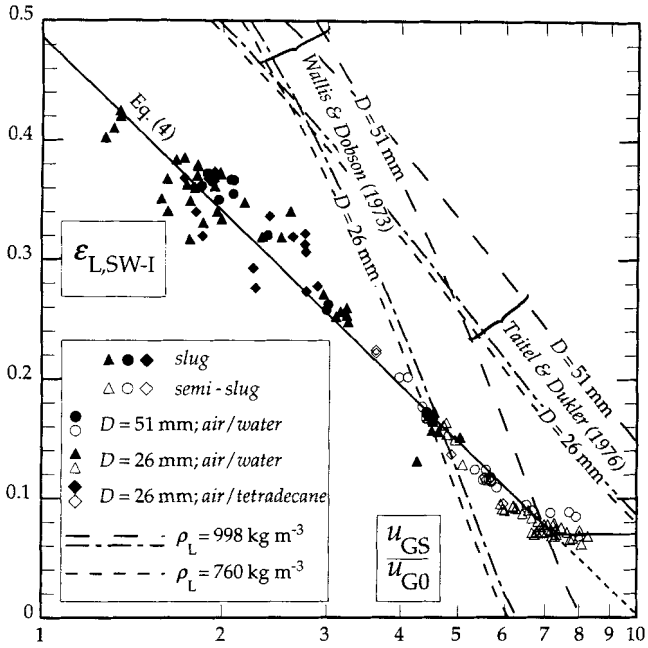

Figure 1. Liquid holdup at the stratified-wavy-to-intermittent flow-pattern transition, as a function of u_{GS}/u_{G0}, showing modeled lines and measured points.

pipe, $u_{G0} \approx 1.26$ m·s^{-1}, so that $\epsilon_{L,SW-I} \approx \epsilon_{L0}$, when $u_{GS} \approx 1.26$ m·s^{-1}.

Equation 4 and Figure 1, show that the liquid holdup at marginal stability decreases with increasing gas flow rate. Above a certain value of the superficial gas velocity ($u_{GS} \geq 10u_{G0}$), the flow is unstable for all values of the liquid holdup ϵ_L. Under these conditions, the liquid contents of the pipe are insufficient to sustain intermittent flow, but the gas velocity is sufficiently high to permanently destabilize all interfacial waves. For horizontal flow, instabilities of this type have been reported before (Taitel and Dukler, 1976), and are generally recognized to cause annular flow at sufficiently low liquid holdup. From visual observation, this type of annular flow is characterized by liquid droplets running along the "dry" part of the pipe wall. Therefore, we prefer to call this the *unclosed* annular flow regime. At higher gas and/or liquid flow rates, the annular liquid ring is complete, and *closed* annular flow is obtained. The *lowest* value of the liquid holdup for which intermittent, instead of *unclosed* annular flow was observed is equal to $\epsilon_L \approx 0.07$.

The definition of the critical liquid holdup for flow-pattern transition is only part of the requirement for the prediction of onsetting intermittent flow. In addition, an accurate model for the calculation of the steady-state liquid holdup is indispensable. For this purpose, the modified apparent rough surface (MARS) model of Grolman (1994) performs well, up to the SW-I flow-pattern boundary. The model provides estimates of liquid holdup and pressure gradient that are accurate within an average relative error of 10%. Comparable accuracies are *not* achieved when other, more common models for the liquid holdup are used. The MARS model is summarized in Appendix A.

Experiments

Measuring equipment

The experiments were performed in carefully aligned, slightly inclined glass pipes of 26 mm ($L = 11$ m) and 51 mm ($L = 15$ m) diameter, using *water-saturated air/water* and *air/tetradecane* systems at atmospheric pressure. The approximate transport properties of the gas–liquid systems used are $\rho_G \approx 1.18$ kg·m^{-3}, $\eta_G \approx 1.8\ 10^{-5}$ Pa·s; *demineralized water*: $\rho_L \approx 998$ kg·m^{-3}, $\eta_L \approx 10^{-3}$ Pa·s, $\sigma \approx 0.072$ Pa·m; and *tetradecane*: $\rho_L \approx 762$ kg·m^{-3}, $\eta_L \approx 2.1\ 10^{-3}$ Pa·s, $\sigma \approx 0.028$ Pa·m. A diagram of the experimental setup is shown in Figure 2. The *volumetric gas-flow rate*, relevant *temperatures*, the *weight* of the liquid to be injected into the pipe and the weight of the liquid collected at the pipe, were sampled at frequencies of 0.2, 0.1 and 5 Hz respectively, and recorded. The gas-flow rate was measured with an Instromet turbine meter ($\pm 0.5\%$), the temperatures with Pt-100 thermometers (± 0.05 K) and the weights with digital Mettler PM-16 and PM-30 precision balances (± 0.5 g). The pipe was positioned at *ten* different angles of inclination ($\pm 0.005°$), using two specially designed angle gauges, one at each end. The experiments were performed isothermally (± 1 K) at room temperature.

Measuring procedures

At the start of every experiment, the gas flow rate was set to its initially desired value and the inlet temperature of the saturated air was adjusted to ≈ 1 K below that of the surroundings, to avoid downstream condensation. After some time, the flow of liquid into the pipe was activated and the system allowed to attain a steady state. Subsequently, the superficial gas velocity was slowly decreased by 0.1 10^{-3} to 0.5 10^{-3} m·s^{-2} near the SW-I transition, until intermittent flow occurred. In addition to visual observation of intermittent flow, its onset was also evident from oscillations in the measured liquid holdup and superficial velocities, which were displayed on a computer screen. During periods of steady-state stratified-wavy flow, measurements of the other flow variables, such as the pressure gradient, were performed. At the end of a run, the entrance liquid flow was shut off and the liquid from the pipe was quantitatively collected. The liquid holdup and gas and liquid flow rates at the moment of instability were obtained by tracing back in the signals recorded. The ability to do so was imperative, since after flow-pattern transition, the highly transient nature of flow rates and system pressure prohibits accurate measurement of these variables.

Results

The relative absence of waves in the entrance region ($0 < x < 0.1L$) and the liquid-level gradient in the exit region ($0.85L < x < L$) tend to stabilize the stratified-wavy flow, and slugs were never observed to form in these zones. However, all other positions in the pipe appear to have an equal chance of becoming the source of the initial slug or semislug that marks the transition to intermittent flow. From the random axial distribution of these initial instabilities, it is clear that the transition studied is not an entrance effect, nor is it likely to be caused by local imperfections in the test rig.

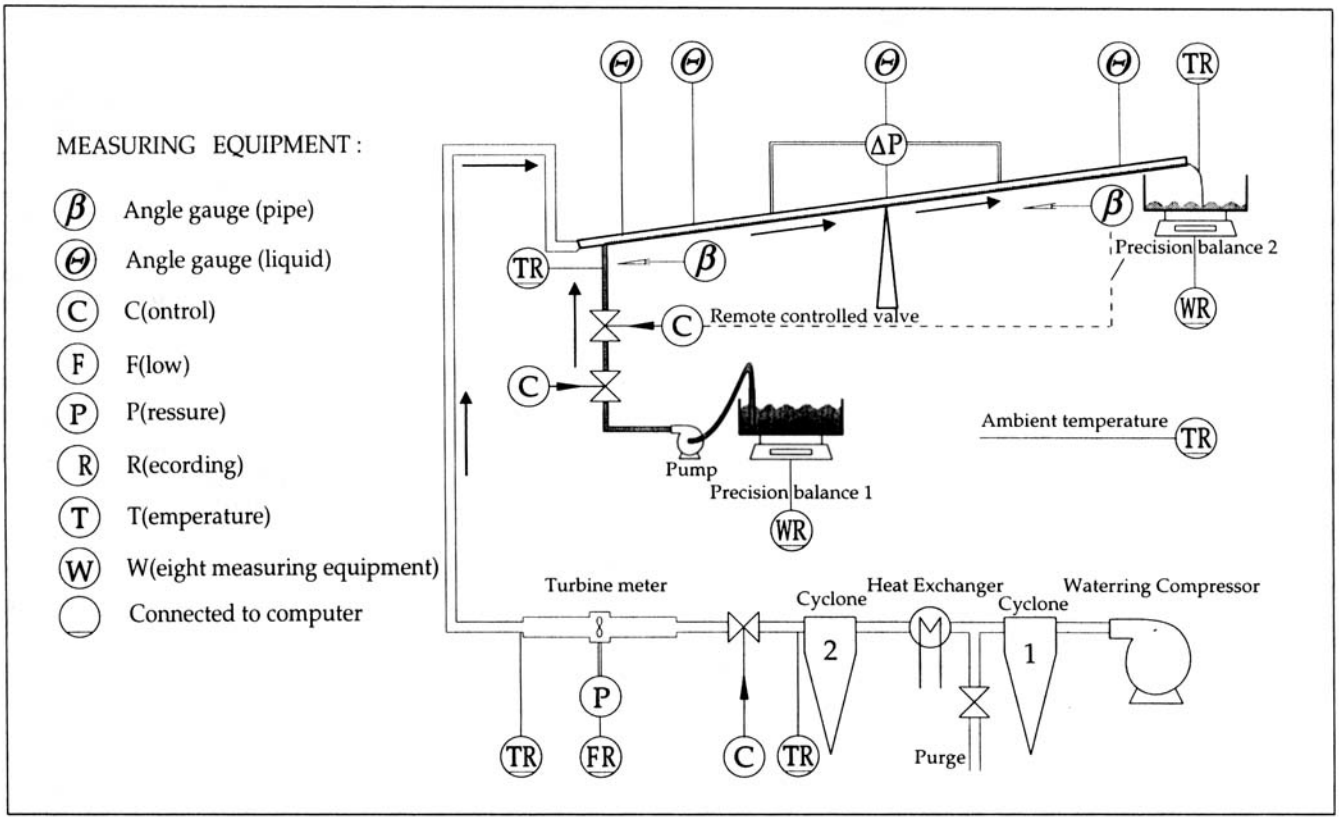

Figure 2. Diagram of the experimental setup.

Assessment of models

Figure 1 shows $\epsilon_{L,\text{SW-I}}$, the average liquid holdup measured at the unstable conditions leading to flow-pattern transition, as a function of u_{GS}/u_{G0}. The solid line in Figure 1 shows $\epsilon_{L,\text{SW-I}}$ according to Eq. 4. Other, dashed lines show the stability criteria of Wallis and Dobson (1973; Eq. 1, assuming $u_L/u_G \ll 1$) and Taitel and Dukler (1976; Eq. 2). A total of 1,270 sets of measurements were performed close to the SW-I transition boundaries, at 10 angles of inclination, using two pipe diameters and two gas–liquid systems. In Figure 1 only the values of 135 sets of *unstable* measurements, which evolved into a flow-pattern transition, are displayed. The stable, stratified-wavy flow regime lies below the solid line in Figure 1; intermittent flow is encountered above the line, at conditions of higher liquid holdup. The boundary is valid when it is approached from the wavy, low ϵ_L side only, since the SW-I transition may be subject to a hysteresis effect. Therefore the requirement for stability of stratified-wavy flow is that the *steady-state* liquid holdup is smaller than the *critical* liquid holdup, that is, $\epsilon_L < \epsilon_{L,\text{SW-I}}$.

The horizontal line in Figure 1 at $\epsilon_{L,\text{SW-I}} = 0.07$ marks the liquid holdup values below which the amount of liquid in the pipe is insufficient to sustain intermittent flow. Hence, the stability line according to Eq. 4 is dashed for $\epsilon_{L,\text{SW-I}} < 0.07$. Figure 1 demonstrates that the modeled SW-I boundary marks the transition from wavy to both slug (solid markers) and semislug flow (open markers). The exact conditions for which slug flow prevails above semislug flow were not investigated.

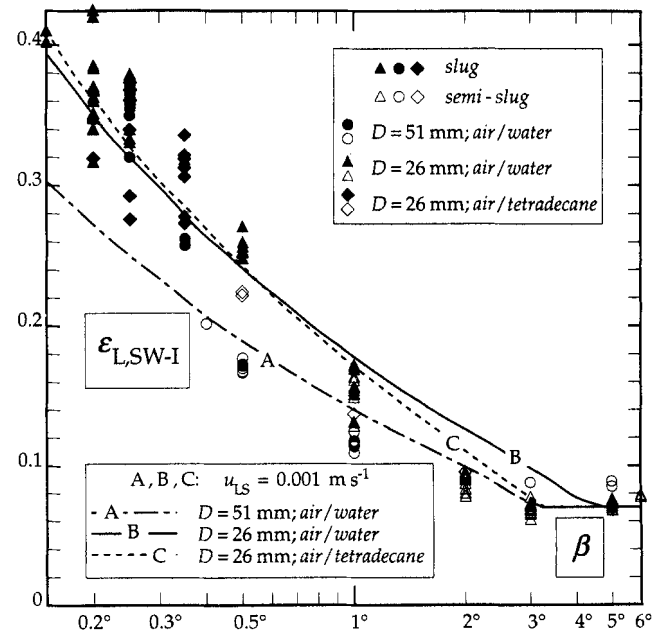

Figure 3. Liquid holdup at the stratified-wavy-to-intermittent flow-pattern transition, as a function of the inclination angle β, showing modeled lines at $u_{LS} = 10^{-3}$ m·s^{-1} and measured points [$3\times10^{-4} < u_{LS}/(\text{m}\cdot\text{s}^{-1}) < 2\times10^{-2}$].

In Figure 3, $\epsilon_{L,SW\text{-}I}$ is plotted as function of the angle of inclination β, and contains the same experimental data as in Figure 1. Figure 3 also shows model lines for $\epsilon_{L,SW\text{-}I}$ at a superficial liquid velocity of $u_{LS} = 10^{-3}$ m·s^{-1}, calculated with Eq. 4 and the MARS model from Appendix A. It is clear that Figure 1 accommodates significant effects of diameter and angle of inclination on $\epsilon_{L,SW\text{-}I}$, which become apparent in Figure 3.

Flow-pattern maps

Figure 1 in fact is a flow pattern map for the SW-I transition in slightly inclined gas–liquid pipe flow. However, before the current flow pattern can be predicted from Figure 1, the steady-state liquid holdup must be calculated. Since the liquid holdup varies significantly with the gas and liquid flow rates, angle of inclination, pipe diameter, and transport properties, Figure 1 is not easily interpreted. Flow-pattern maps are presented in Figures 4 to 9, on the familiar u_{LS} vs. u_{GS} axes. These figures show modeled lines and measured points for the (arbitrarily chosen) angles of inclination of 0.5° and 1.0°, for *air/water* flow in a 26-mm-dia. pipe (Figures 4 and 5), *air/water* flow in a 51-mm-diameter pipe (Figures 6 and 7), and *air/tetradecane* flow in a 26-mm-diameter pipe (Figures 8 and 9). The bold lines marked SW-I represent the SW-I flow-pattern boundary, calculated with Eq. 4 and the MARS model for the steady-state liquid holdup. The bold, dashed line in Figures 4 to 9 represents an extrapolation of the SW-I boundary into the region of $\epsilon_{L,SW\text{-}I} < 0.07$, and

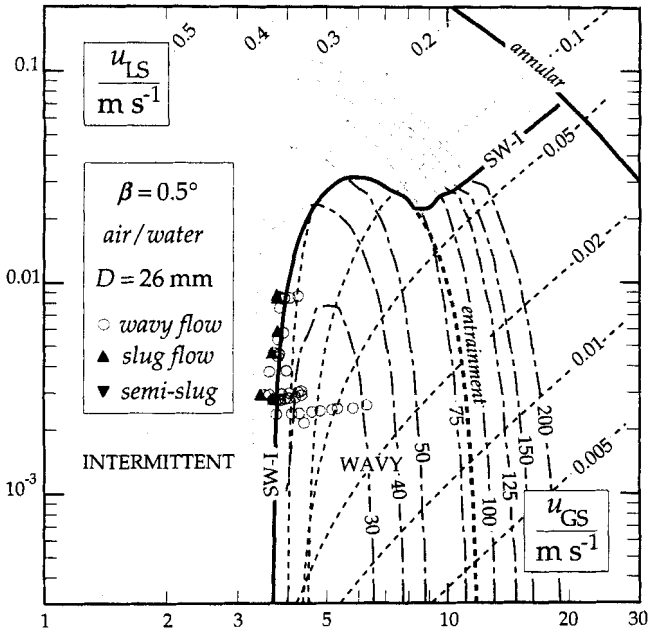

Figure 4. Flow pattern map with boundaries of stratified-wavy, intermittent, and annular flow, showing calculated lines of constant liquid holdup ($0.005 \le \epsilon_L \le 0.50$) and constant pressure gradient [$30 \le (-dP/dL)/(\text{Pa}\cdot\text{m}^{-1}) \le 200$].

The markers represent completed experiments, for which there is generally less than 10% difference between the measured and calculated values of liquid holdup and pressure gradient.

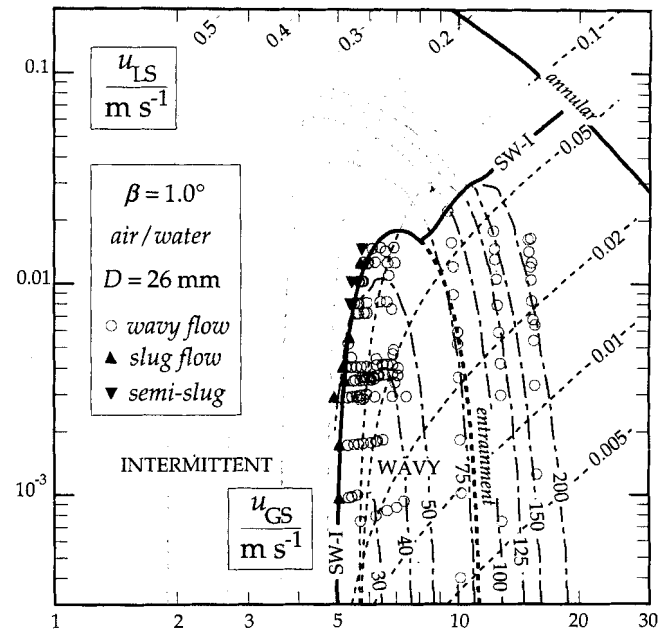

Figure 5. See caption of Figure 4.

marks the onset of wave instabilities and entrainment for higher gas flow rates.

The lines marked "annular" follow from the condition that the wetted wall fraction $\theta = 0.8$ (see the Appendix). Values of the wetted wall fraction between 0.8 and 1.0 are not observed in gas–liquid pipe flow, due to hysteresis effects in closing and opening the annular liquid ring (Hart et al., 1989). Furthermore, Figures 4 to 9 show lines of constant liquid holdup ($0.005 \le \epsilon_L \le 0.5$) and lines of constant pressure gradient [$30 \le (-dP/dL)/(\text{Pa}\cdot\text{m}^{-1}) \le 200$] calculated with the MARS model, which serve to demonstrate the variation of the liquid holdup and the pressure gradient with the superfi-

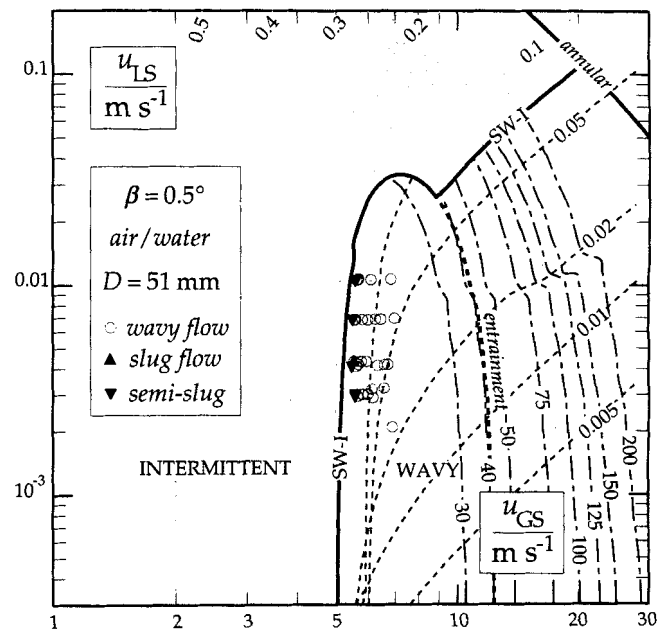

Figure 6. See caption of Figure 4.

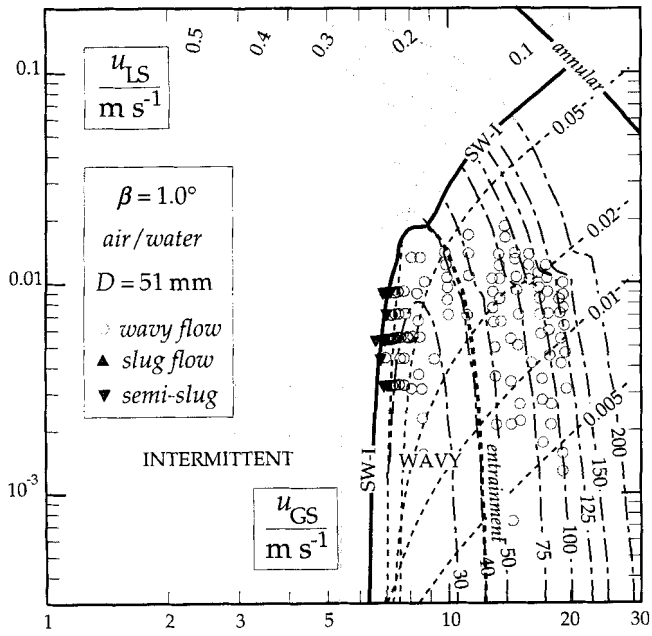

Figure 7. See caption of Figure 4.

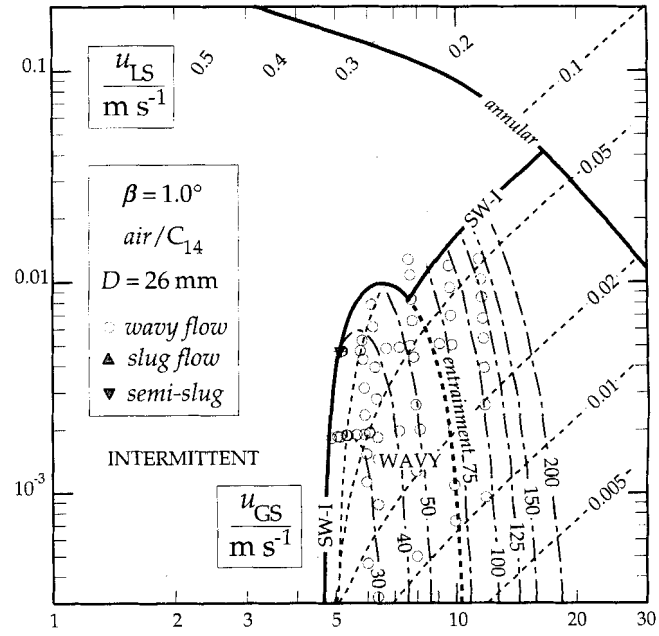

Figure 9. See caption of Figure 4.

cial gas and liquid velocities. The gray lines are extrapolations into the intermittent flow regime. The MARS model predictions of liquid holdup and pressure gradient are, on average, accurate within 10% for all our measurements (Grolman, 1994). Therefore the modeled lines of constant ϵ_L and constant $-dP/dL$ in Figures 4 to 9 have effectively been verified by the experiments represented by the markers.

Discussion of Results in Relation to Existing Models

The semitheoretical models of Wallis and Dobson (1973) and Taitel and Dukler (1976), based on horizontal flow, are representative of a widely used prediction method for the SW-I transition boundary in gas–liquid flow. Figure 1 shows that there are significant differences between the models based on horizontal flow and our model obtained with measurements from *inclined* pipes. Having measured the average liquid holdup and superficial gas velocity accurately and simultaneously, the significant differences in outcome still remain to be resolved.

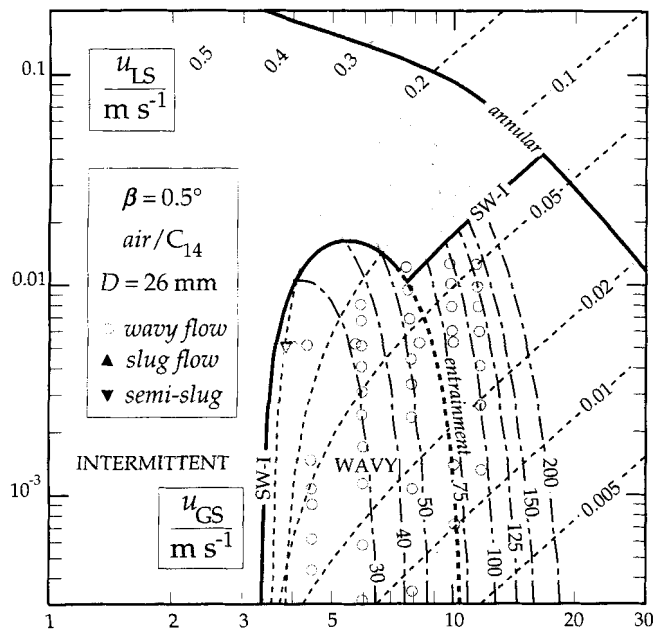

Figure 8. See caption of Figure 4.

Based on their extensive linear stability analysis for horizontal pipes, Lin and Hanratty (1986) presented h_L/D, the dimensionless liquid level, as a function of $u_{GS}\{\rho_G/(\rho_L g D)\}^{0.5}$ on semilogarithmic axes. Although these graphs are somewhat similar to ours, the diameter and friction-factor dependencies are quite different. In addition, Hanratty (1991) concludes that a diameter effect of $D^{-0.5}$ is rather too strong, leading to implausible values of u_{GS} for large pipes. Indeed, our results suggest a smaller $D^{-0.125}$ dependency for inclined gas–liquid pipe flow.

Stability criteria based on wave considerations (Wallis, 1969; Barnea and Taitel, 1993) require partial derivatives of frictional terms with respect to liquid holdup to be calculated. Since these theoretical criteria are very elegant, we regret that a satisfactory description of the results with these methods could not be obtained. The major difficulty appears to be modeling the *local* variation of shear stresses and pressure with the local holdup and flow rates. Apparently, average friction factors and average liquid holdup are not a good substitute for their local counterparts.

Our experiments demonstrate that supercritical flow is *not* required for the inception of slugs in inclined flow. This can be envisioned by considering that in cocurrent, inclined gas–liquid pipe flow, lowering the superficial gas velocity is always sufficient to cause slugs, provided $\beta > \arcsin(D/L)$. It leads to the fundamental question of whether the mechanisms causing slugs in inclined flow are different from those in horizontal flow, or whether supercritical flow is not a prerequisite for slugs in horizontal flow either.

Effects of D and β on $\epsilon_{L,SW\text{-}I}$

A total of 1,270 experiments, at 10 angles of inclination ($0.1° \leq \beta \leq 6.0°$), two pipe diameters, and two gas–liquid systems, have elucidated the SW-I transition boundaries in slightly inclined gas–liquid pipe flow. Because the average liquid holdup and superficial velocities were measured simultaneously, the conditions of flow-pattern transition were established independently from friction-factor and liquid holdup models. These results prove that the liquid holdup plays a central role in determining stability. *Therefore, reliable a priori estimates of the flow pattern can only be obtained with an accurate model for the steady-state liquid holdup.* In inclined pipes close to the SW-I boundaries, ϵ_L is extremely sensitive to small changes in u_{GS} (Figures 4 to 9). For the prediction of the liquid holdup under the conditions investigated, the MARS model from Appendix A is the only accurate estimation method currently available. Therefore, the MARS model is an integral part of the flow-pattern prediction method presented.

The study shows that small angles of inclination can have a marked effect on the flow pattern in gas–liquid pipe flow, at reduced superficial gas velocities. The liquid holdup at the SW-I transition is higher for the smaller angles of inclination β, as can be judged from Figure 3. Due to the large amount of liquid in the pipe, high liquid holdup values prior to instability result in large initial slugs. Therefore, in pipelines containing sections at small angles of inclination, severe slugs must be anticipated when the flow rate of the gas is reduced below the critical value. At larger angles of inclination, the combination of a larger critical gas flow rate and a smaller critical liquid holdup cause smaller, or just semislugs to appear at the SW-I boundary (Figures 1 and 3).

In gas–liquid pipe flow at *very* small angles of inclination, the formation of slugs may be inhibited when the raise in elevation from start to end is less than one pipe diameter, that is, $\beta < \arcsin(D/L)$. This is due to gravity-induced interfacial liquid-level gradients, which may be sufficient to propel the liquid through the pipe, especially at small liquid flow rates.

Comparing Figures 4 and 5 with Figures 6 and 7, respectively, shows that the critical superficial gas velocity is *increased* by increasing the pipe diameter. Therefore, in designing pipes for inclined gas–liquid flow with a given duty, care must be taken not to select pipe diameters that are too large, if slugs are to be avoided. Rather, it may be sensible to be content with some increased pressure gradient and a smaller diameter pipe, to stay on the safe side of the SW-I transition boundary.

Conclusions

- The liquid holdup at the SW-I (slug or semislug) flow-pattern transition $\epsilon_{L,SW\text{-}I}$ in slightly inclined pipes follows from

$$\epsilon_{L,SW\text{-}I} = 0.486 - 0.21 \ln \frac{u_{GS}}{u_{G0}}; \qquad 0.07 < \epsilon_{LSW\text{-}I} < 0.45$$

in which $u_{G0} \equiv \{\nu_G^2(\rho_L/\rho_G - 1)^3 g^3 D\}^{1/8}$. If $\epsilon_{L,SW\text{-}I} < 0.07$, no intermittent flow occurs.

- The necessary and sufficient condition for stable, steady-state separated gas–liquid flow in upward inclined pipes is $\epsilon_L < \epsilon_{L,SW\text{-}I}$. The steady-state liquid holdup ϵ_L, up to the SW-I boundary, can be calculated with the MARS model from Appendix A, using the values of 10 relevant physical quantities (u_{GS}, u_{LS}, ρ_G, ρ_L, η_G, η_L, σ, D, β, and g).
- The transition stratified-wavy-to-annular (SW-A), that is, from stratified-wavy to *closed* annular flow, is obtained from the MARS model, using the condition $\theta = 0.8$. Closed annular flow is obtained for $\theta \geq 0.8$, while for $\theta < 0.8$, either *unclosed* annular, stratified-wavy, or intermittent flow may occur.

Acknowledgments

The authors are grateful for the financial support by The Netherlands Foundation for Chemical Research (SON), The Netherlands Technology Foundation (STW), Shell Research B.V. (Amsterdam, The Netherlands), Energiebeheer Nederland/DSM (Heerlen, The Netherlands), and Gasunie N.V. (Groningen, The Netherlands).

Notation

Fn = friction number, Eq. A12, 1
res = residue, defined in Eq. A17, $\mathrm{Pa \cdot m^{-1}}$
Re = Reynolds number; $\rho u D/\eta$, 1
x = axial coordinate of a point in the pipe, m
ρ = density, $\mathrm{kg \cdot m^{-3}}$

Subscripts

0 = physical constant, Eq. 4
max = physically attainable maximum in magnitude

Literature Cited

Barnea, D., and Y. Taitel, "Transient Formulation Modes and the Stability of Steady-State Annular Flow," *Chem. Eng. Sci.*, **44**, 325 (1989).

Barnea, D., and Y. Taitel, "Kelvin–Helmholtz Stability Criteria for Stratified Flow: Viscous versus Non-Viscous (Inviscid) Approaches," *Int. J. Multiphase Flow*, **19**, 639 (1993).

Bruno, K., and M. J. McCready, "Processes Which Control the Interfacial Wave Spectrum in Separated Gas-Liquid Flows," *Int. J. Multiphase Flow*, **15**, 531 (1989).

Grolman, E., *Gas-Liquid Flow with Low Liquid Loading in Slightly Inclined Pipes*, PhD Thesis, Univ. of Amsterdam, Amsterdam, The Netherlands (1994).

Eck, B., *Technische Strömungslehre*, Springer-Verlag, New York (1973).

Hanratty, T. J., "Separated Flow Modelling and Interfacial Transport Phenomena," *Appl. Sci. Res.*, **48**, 353 (1991).

Hart, J., P. J. Hamersma, and J. M. H. Fortuin, "Correlations Predicting Frictional Pressure Drop and Liquid-Holdup During Horizontal Gas-Liquid Pipe Flow with a Small Liquid Holdup," *Int. J. Multiphase Flow*, **15**, 947 (1989).

Helmholtz, H., "Über discontinuirliche Flüssigkeitsbewegungen," *Monatsberg. Akad. Wiss. Berlin*, 215 (1868).

Kelvin, "Hydrokinetic Solutions and Observations," *Phil. Mag.*, **4**, 374 (1871).

Kordyban, E., and T. Ranov, "Mechanisms of Slug Formation in Horizontal Two-Phase Flow," *Trans. ASME J. Basic Eng.*, **92**, 857 (1970).

Kordyban, E., "The Transition to Slug Flow in the Presence of Large Waves," *Int. J. Multiphase Flow*, **3**, 603 (1977).

Lin, T. F., and T. J. Hanratty, "Prediction of the Initiation of Slugs with Linear Stability Theory," *Int. J. Multiphase Flow*, **13**, 549 (1986).

Mishima, K., and M. Ishii, "Theoretical Prediction of Onset of Horizontal Slug Flow," *J. Fluids Eng.*, **102**, 441 (1980).

Nikuradse, J., "Strömungsgesetze in Rauhen Rohren: VDI Forschungsheft 361," *Beil. Forsch. Geb. Ingenieurwes. B*, **4**, 62 pp. (1933).
Taitel, Y., and A. E. Dukler, "A Model for Predicting Flow Regime Transitions in Horizontal and Near Horizontal Gas-Liquid Flow," *AIChE J.*, **22**, 47 (1976).
Taitel, Y., and A. E. Dukler, "A Model for Slug Frequency during Gas-Liquid Flow in Horizontal and Near Horizontal Pipes," *Int. J. Multiphase Flow*, **3**, 585 (1977).
Wallis, G. B., *One-Dimensional Two-Phase Flow*, Chap. 4, McGraw Hill, New York (1969).
Wallis, G. B., and J. E. Dobson, "The Onset of Slugging in Horizontal Stratified Air-Water Flow," *Int. J. Multiphase Flow*, **1**, 173 (1973).

Appendix A: MARS Model

Momentum balance equations

The modified apparent rough-surface model enables one to calculate the average liquid holdup ϵ_L and the average pressure gradient $(-dP/dL)$ for gas–liquid pipe flow from a set of 10 relevant physical quantities, that is, the superficial velocities and transport properties of gas and liquid (u_{GS}, u_{LS}, ρ_G, ρ_L, η_G, η_L, σ), the diameter and angle of inclination of the pipe (D, β), and the gravitational acceleration (g). The MARS model can be applied to separated gas–liquid flow, that is, to the stratified-smooth, stratified-wavy, and annular flow regimes. The model is based on the following momentum balance equations for steady-state, separated, cocurrent gas–liquid pipe flow:

$$A_G\left[-\frac{dP}{dL}\right]_G = \tau_{GW}S_G + \tau_i S_i + A_G\rho_G g\sin(\beta) \quad \text{(A1)}$$

$$A_L\left[-\frac{dP}{dL}\right]_L = \tau_{LW}S_L - \tau_i S_i + A_L\rho_L g\sin(\beta) \quad \text{(A2)}$$

containing three cross-sectional areas

$$A_{\text{tot}} = \pi D^2/4; \quad A_L = \epsilon_L A_{\text{tot}}; \quad A_G = (1-\epsilon_L)A_{\text{tot}} \quad \text{(A3)}$$

three perimeters

$$S_i = s_i\pi D; \quad S_L = \theta\pi D; \quad S_G = (1-\theta)\pi D \quad \text{(A4)}$$

three shear stresses

$$\tau_{GW} = f_G\frac{1}{2}\rho_G\frac{u_{GS}^2}{(1-\epsilon_L)^2}; \quad \tau_{LW} = f_L\frac{1}{2}\rho_L\frac{u_{LS}^2}{\epsilon_L^2};$$

$$\tau_i = f_i\frac{1}{2}\rho_G\left\{\frac{u_{GS}}{(1-\epsilon_L)} - u_i\right\}^2. \quad \text{(A5)}$$

The dimensionless perimeters s_i $(= S_i/\pi D)$ and θ $(= S_L/\pi D)$ and the friction factors f_i, f_G, and f_L are empirical functions of relevant physical quantities in gas–liquid pipe flow. The empirical correlations are based on the results of 2500 experiments, covering gas–liquid pipe flow with two distinct gas–liquid systems, three pipe diameters (15, 26, and 51 mm), and fourteen small angles of inclination $(-3° \le \beta \le +6°)$.

Special attention was paid to the correlation for the interfacial friction factor f_i, which is assumed to be a function of the equivalent relative (sand) roughness k/D (Nikuradse, 1933) of the gas–liquid interface and *Reynolds* number of the gas phase. The value of the relative roughness k was found not be a direct function of the ten *primary* relevant physical quantities, but also of the *secondary* quantities s_i, θ, and ϵ_L, mainly because k is closely, but not directly, related to the average liquid-layer thickness. Therefore, both f_i and ϵ_L need to be calculated in an iterative process.

Determination of ϵ_L

The following procedure is used to calculate the liquid holdup ϵ_L: (1) a first estimate of ϵ_L is required, for which the Hart et al. (1989) model is employed:

$$\text{estimate: } \frac{\epsilon_L}{1-\epsilon_L} = \frac{u_{LS}}{u_{GS}}\left\{1+\left(\frac{\rho_L}{\rho_G}108Re_{LS}^{-0.726}\right)^{0.5}\right\};$$

$$Re_{LS} = \frac{\rho_L u_{LS} D}{\eta_L}. \quad \text{(A6)}$$

The dimensionless perimeters θ and s_i are calculated from (Grolman, 1994):

$$\theta = \theta_0\left(\frac{\sigma_{\text{water}}}{\sigma}\right)^{0.15} + \frac{\rho_G}{(\rho_L-\rho_G)}\frac{1}{\cos(\beta)}\left\{\frac{\rho_L u_{LS}^2 D}{\sigma}\right\}^{0.25} \times\left\{\frac{u_{GS}^2}{(1-\epsilon_L)^2 gD}\right\}^{0.8} \quad \text{(A7)}$$

$$s_i = \frac{S_i}{\pi D} = \frac{\theta-\theta_0}{1-\theta_0}(1-\epsilon_L)^{0.5} + \frac{1-\theta}{1-\theta_0}\frac{\sin(\pi\theta_0)}{\pi}, \quad \text{(A8)}$$

in which the minimum wetted wall fraction θ_0 is approximated by

$$\theta_0 \approx 0.624\epsilon_L^{0.374}; \quad \text{(A9)}$$

(2) The gas-phase smooth-pipe friction factor f_G and the interfacial friction factor f_i are calculated from (Eck, 1973)

$$f_G = \frac{0.07725}{\{\log_{10}[Re_G/7]\}^2}; \quad Re_G = \frac{\rho_G u_{GS} D}{\eta_G(1-\theta+s_i)}; \quad \text{(A10)}$$

$$f_i = \frac{0.0625}{\left\{\log_{10}\left(\frac{15}{Re_G} + \frac{k}{3.715D}\right)\right\}^2}. \quad \text{(A11)}$$

The equivalent relative sand roughness k/D is calculated using the following two equations (Grolman, 1994):

$$Fn = \frac{f_i}{(0.05 + f_i)(1 - \epsilon_L)^{1.5}} \left(\frac{u_{GS}}{\sqrt{gD}} \right) \left(\frac{\sigma}{\eta_L \sqrt{gD}} \right)^{0.04} \times \left(\frac{\rho_L g D^2}{\sigma} \right)^{0.22} \quad \text{(A12)}$$

$$\frac{k}{D} = 0.5145 \epsilon_L s_i^{-1.5} \{\tanh[0.05762(Fn - 33.74)] + 0.9450\}. \quad \text{(A13)}$$

Equation A12 contains the interfacial friction factor, which must follow from Eq. A11. Therefore, f_i is calculated *iteratively* from Eqs. A11 to A13, using $k/D = 0$ for a first estimate of Eq. A11.

(3) The liquid-phase friction factor f_L is calculated from (Grolman, 1994; Hart et al., 1989)

$$f_L = f_i \; 202 \left(\frac{\eta_{\text{water}}}{\eta_L} \right)^{0.274} \theta_0 Re_{LS}^{-1} Re_G^{0.25}; \quad \frac{Re_{LS}}{\theta} < 2{,}100 \quad \text{(A14)}$$

$$f_L = f_i \; 108 Re_{LS}^{-0.726}; \quad \frac{Re_{LS}}{\theta} \geq 2{,}100. \quad \text{(A15)}$$

Note that by defining the hydraulic diameter in the usual way, $Re_L = Re_{LS}/\theta$.

(4) The average interfacial velocity u_i follows from (Grolman, 1994)

$$u_i = \frac{1.8 u_{LS}}{\epsilon_L} \text{ if } \frac{Re_{LS}}{\theta} < 2{,}100 \text{ and}$$

$$u_i = \frac{u_{LS}}{\epsilon_L} \text{ if } \frac{Re_{LS}}{\theta} \geq 2{,}100. \quad \text{(A16)}$$

For steady-state gas–liquid pipe flow, in the absence of interfacial liquid-level gradients, the axial pressure gradients in the gas and liquid phase are equal. Therefore, Eqs. A1 and A2 yield

$$res = \tau_{LW} \frac{S_L}{A_L} - \tau_{GW} \frac{S_G}{A_G} - \tau_i S_i \left\{ \frac{1}{A_L} + \frac{1}{A_G} \right\} + (\rho_L - \rho_G) g \sin(\beta) \underset{\text{state}}{\overset{\text{steady}}{=\!=}} 0. \quad \text{(A17)}$$

The value of *res* is calculated repeatedly with Eqs. A5–A17 while ϵ_L is varied. This procedure is repeated until the closest solution to $res = 0$, within a specified accuracy of ϵ_L, is obtained

Determination of (− dP/dL)

The axial pressure gradient is obtained from Eq. A1:

$$\left[-\frac{dP}{dL} \right] = \tau_{GW} \frac{S_G}{A_G} + \tau_i \frac{S_i}{A_G} + \rho_G g \sin(\beta) \quad \text{(A18)}$$

after substitution of the relevant values calculated in the preceding section.

Flow-pattern map

The procedure just listed yields values of ϵ_L and $-dP/dL$ for every combination of the ten relevant primary physical quantities. In a flow-pattern map, lines of constant liquid holdup, lines of constant pressure gradient, and lines of marginal stability, that is, $\epsilon_L = \epsilon_{L,\text{SW-I}}$, can now be constructed.

Manuscript received July 19, 1994, and revision received July 3, 1995.